Draft version October 25, 2017
Typeset using LaTeX **twocolumn** style in AASTeX61

RELATING THE REIONIZATION TIMES OF GALAXIES TO THEIR PRESENT HALO MASSES

Dominique Aubert,[1] Pierre Ocvirk,[1] Nicolas Deparis,[1] INCITE,[1] and CLUES[1]

[1] *Observatoire Astronomique de Strasbourg*
11 rue de l'Universite
67000, Strasbourg, France

Submitted to ApJL

ABSTRACT

Todays galaxies experienced cosmic reionization at different times in different locations, since reionization was inhomogeneous. We show this by deriving the reionization redshifts of the intergalactic medium surrounding their progenitors, using fully-coupled radiation-hydrodynamics simulation of galaxy formation and reionization at z ¿ 6, matched to N-body simulation to z = 0. Constrained initial conditions were chosen to form the well-known structures of the local universe, including the Local Group and Virgo, in a (91 Mpc)^3 volume large enough to model both global and local reionization. Reionization simulation CoDa I-AMR, by hybrid CPU-GPU code EMMA, used $(2048)^3$ particles and $(2048)^3$ initial cells, adaptively-refined, while N-body simulation CoDa I-DM2048, by Gadget2, used $(2048)^3$ particles, to find these reionization times for all galaxies at z = 0 from 10^8 to $10^{14} M_\odot$. Galaxies with $M(z=0) > 10^{11} M_\odot$ reionized earlier than the universe as a whole, by up to 500 Myrs, with significant scatter. For Milky-Way-like galaxies, reionization redshifts ranged from 8 to 15, while global reionization ended at 6.1. Galaxies with $M(z=0) < 10^{11} M_\odot$, however, typically reionized as late or even later than global reionization, in neighborhoods where reionization was completed by external radiation. The duration of reionization was sometimes substantial, ranging as large as the range of reionization times. The Milky Way and M31 reionized earlier than global reionization, neither dominated by external radiation; tracking their progenitors using either halos or particles yielded z = 9.8 (MW) and 11 (M31) or z = 8.2 (both), respectively.

Keywords: dark ages, reionization, first stars — galaxies: high-redshift — methods: numerical

Corresponding author: Dominique Aubert
dominique.aubert@astro.unistra.fr

1. INTRODUCTION

The emergence of a UV radiation field during the Reionization sets the thermal and ionisation state of the intergalactic medium. It also suppresses star formation in the progenitors of galaxies through photo-heating especially low-mass objects below $10^9 M_\odot$. Accordingly, reconstructed star formation histories of the faintest dwarf galaxies indicate that the Reionization slowed down the build up of their stellar populations (see e.g. Brown et al. (2014)). Likewise recent radiative hydrodynamics simulations could reproduce this suppression in large high resolution simulations (Ocvirk et al. 2016).

The Reionization is not a uniform and instantaneous process: the structure of the density field translates into an heterogeneous distribution of sources and absorbers. Different patches and objects in the Universe do not reionize at the same time, but have widely ranging reionization redshifts.

The timing of the Reionization can have an impact on e.g. the satellite populations of z=0 galaxies (see e.g. Koposov et al. (2009); Busha et al. (2010); Ocvirk & Aubert (2011); Iliev et al. (2011); Ocvirk et al. (2014); Gillet et al. (2015)) and the assumption on extended or instantaneous reionizations has a dramatic impact on the stellar populations of satellite galaxies. In a global context where the exact contribution of small galaxies to the Reionization is debated (see e.g. Bouwens et al. (2014); Finkelstein et al. (2015)), all these aspects push for an improved description of the transition as seen from the high-z galaxies.

In this letter, we want to determine the timings of the Reionization as experienced by today's galaxies and probe the heterogeneity of process. The main challenge is to connect contemporary objects to the Epoch of Reionization (EoR) : 13 billions years separate the Reionization from today and given the variety of build-up histories, it's not an easy task to determine the reionization context of a $z \ll 6$ galaxy. To assess these questions, we combine for the first time a large scale dark-matter-only CLUES simulation at z=0 with a state-of-the-art AMR radiative hydrodynamics simulation of the EoR, the CODA I -AMR simulation, that self-consistently provides the reionization past of today galaxies. Because they share the same set of initial conditions (IC), these two simulations can be connected and predictions on the time and durations of the Reionization of z=0 galaxies can be made. Furthermore the ICs were constrained to include analogs of the Local Group (LG) in a realistic large-scale environment and allow us to assess how representative is the LG, arguably the best place to assess the past of small and old galaxies.

The work presented here follow the lines of previous studies made by e.g. Weinmann et al. (2007) or Dixon et al. (2017) who used radiative transfer post-processing of pre-existing simulations. It also complements Alvarez et al. (2009) and Li et al. (2014) who focused on scales and masses relevant for massive galaxies or clusters, using a semi-numerical methodology: thanks to the scales explored here ($64h^{-1}$ Mpc box size sampled at a kpc resolution) we focus on smaller objects with masses between $10^8 M_\odot$ and $10^{13} M_\odot$. Our methodology is also similar to Ocvirk et al. (2014) on the LG Reionization. However, the current letter reassess this work by including the LG environment and by comparing it to the full population of galaxies.

We first present our set of simulations and the analysis performed. We then describe the times and duration of reionizations for our simulated population of galaxies before discussing the case of the LG. Future investigations routes are then presented.

2. METHODS

2.1. *Initial Conditions*

The CLUES initial conditions used here assume a WMAP 5 cosmology ($\Omega_m = 0.279, \Omega_v = 0.721, H_0 = 70$ km/s/Mpc, Hinshaw et al. (2009)). They cover a 64 Mpc/h comoving volume with 2048^3 grid cells and particles. The initial phases were chosen to produce an analog of the Local Universe at z=0 (see Gottloeber et al. (2010),Iliev et al. (2011)) providing a Milky Way (MW)-M31 pair with the right mass range and separation in the proper large scale environment. These choices were motivated by future comparisons with the CODA I simulation (Ocvirk et al. 2016) which used the same initial conditions.

2.2. *Simulations*

The $z > 6$ predictions of this project were produced by the AMR simulation code EMMA (Aubert et al. 2015). It tracks the coupled collisionless dynamics, hydrodynamics and radiative transfer and includes standard sub-grid models for star formation and supernovae feedback (Rasera& Teyssier (2006),Deparis et al. (2017), submitted).

Space is sampled on a 2048^3 grid that gets refined if it contains more than 8 DM particles. The grid is prevented to refine to physical resolutions smaller than 500 pc, corresponding to 3 additional levels of refinement by z=6 : the actual number of cells is then multiplied by 2.1, i.e. 18 billions cells.

Star formation is triggered if the gas overdensity in a cell is greater than 50, ensuring that first stellar particles appears at $z \sim 19$: once enabled, the star formation pro-

ceeds according to a Schmidt-Kenicutt Law with an efficiency of 1% (see Rasera& Teyssier (2006),Deparis et al. (2017) subm.). The stellar particles mass is $7 \times 10^4 M_\odot$. They produce ionizing photons according to a Starburst 99 population model (Leitherer et al. 1999) with a Top-Heavy IMF and 0.05 $Z_\odot$ metallicity : the corresponding emissivity is 1.5×10^{17} ionising photons/sec/stellar kg for 3×10^6 years followed by an exponential decrease. Furthermore, an in-situ 20% escape fraction is applied to compute the actual number of photons released in a simulation cell: it ensures a complete reionization at $z \sim 6$. Radiation is propagated using the M1 radiative transfer method with a reduced speed of light $c_{\rm sim} = 0.1$. Mechanical feedback is enabled and a typical energy of 9.8×10^{11} J/stellar kg is released in the surrounding gas after 15×10^6 years: 1/3 via thermal energy, 2/3 via kinetic winds. At z=6, 120×10^6 stellar particles are present.

The CODA I-AMR simulation required 32768 CPUs and 4096 graphics devices (GPUs) on the TITAN (ORNL/DOE) supercomputer. The EMMA code uses GPUs to accelerate the hydrodynamics and the radiative transfer: these modules are respectively 25 and 15 times faster on GPU than a single CPU core.

The CODA I-AMR simulation reached $z = 6$: it presents a reionization epoch consistent with CMB constraints (Planck Collaboration et al. 2015) but with a residual neutral fraction at lower levels than expected from quasars data (Fan et al. (2006), see Fig. 1). The average star formation history is consistent with formation models obtained from the evolution of the high-z UV luminosity function (Bouwens et al. 2014; Finkelstein et al. 2015).

The properties of z=0 halos are obtained from a pure dark-matter Gadget simulation (Springel 2005), using the same initial conditions. Halos were identified using a FOF algorithm with a 0.2 linking length and minimal number of particles of 10, leading to ~ 20 millions structures identified at z=0. The smallest FOF objects detected in the Gadget simulation weighs $2.4 \times 10^7 M_\odot$. Merger trees were also produced to connect z=0 halos to their progenitors during the EoR.

2.3. *Reionization maps*

Reionization maps are built from the ionisation state of hydrogen : this quantity is computed self-consistently in CODA I-AMR and we define the reionization time as the instant when a cell crosses the 0.5 ionized fraction threshold for the first time. The end result is a 3D field, $t_{\rm reion}(x, y, z)$, sampled using 2048^3 pixels corresponding to the base resolution of our simulations (see Fig. 2). When compared to the Gadget halo distribution at z=6,

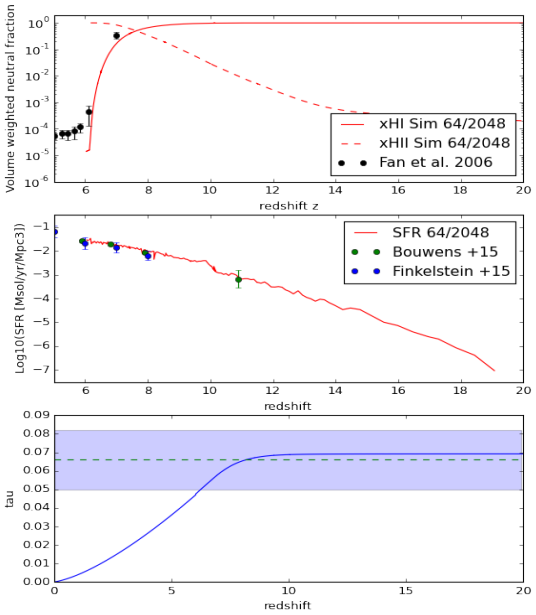

Figure 1. The global average properties of the simulations. From top to bottom : the volume averaged ionization/neutral fraction history, the cosmic star formation rate and the CMB thomson scattering optical depth.

a clear correlation can be seen with the CODA I-AMR reionization map : halos are found at the center of ionization patches and their spatial distribution matches the topology of $t_{\rm reion}(x, y, z)$.

This map is computed on the fly by EMMA with a time resolution driven by hydrodynamical processes. However due to memory management issues, this procedure had to be stopped at z=8 and reionization redshifts were computed from snapshots for the latest stages of the Reionization. At worse the time resolution is 1.4 Myrs at z=6.

Because the simulations do not resolve scales that can be self-shielded, 'galaxy reionization times' should conservatively be understood as 'galaxy environment' times hereafter. Likewise assigning a $t_{\rm reion}$ to a galaxy is in fact assigning this value to patch surrounding this object.

2.4. *Progenitor-based predictions*

This set of predictions is obtained from merger-trees of the DM-only simulation: they give access to $z > 6$ positions $\vec{x}_{\rm mm}$ of the most-massive (mm) progenitors of z=0 halos. Starting from $z = 20$, we look for the earliest step in the merger tree when the most massive progenitor of a halo belongs to an ionized cell. This step has a redshift z_R and the reionization time of a $z = 0$ halo is

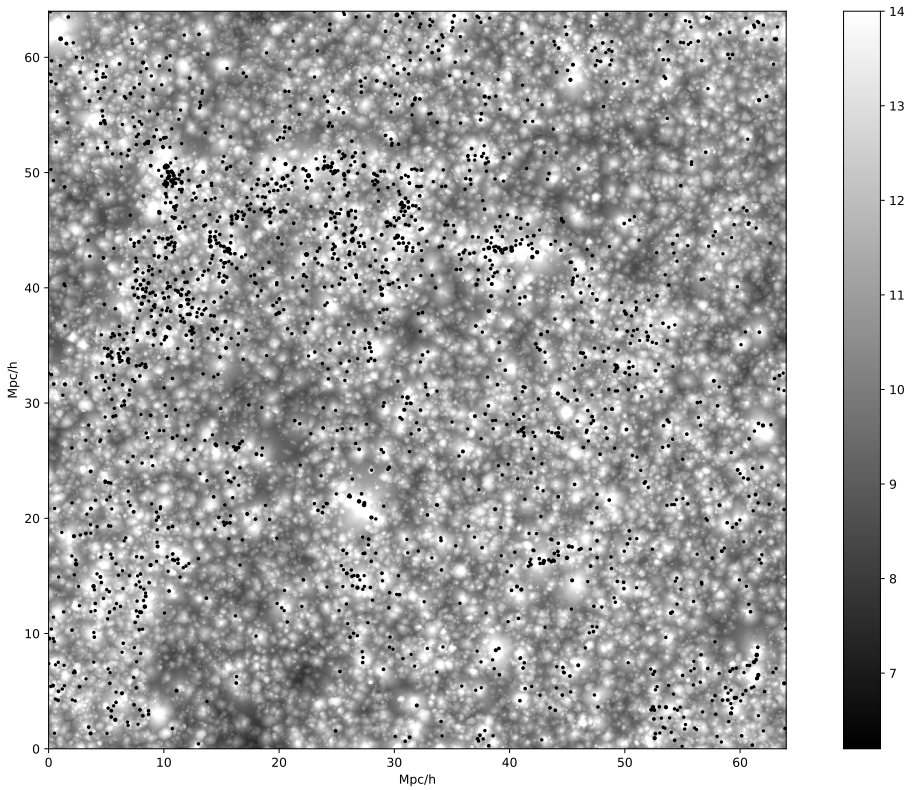

Figure 2. The projected spatial distribution of the 2000 most massive halos from the DM Gadget simulation at z=6 (symbols) and the EMMA maximum value for the reionization redshift found along the projection axis.

given by

$$t_{\rm prog} = t_{\rm reion}(\vec{x}_{\rm mmR}), \quad (1)$$

where $\vec{x}_{\rm mmR}$ is the center-of-mass position of the most massive progenitor of this halo at $z = z_R$.

A halo is assigned a Reionization time only if it has a progenitor at $z > 6$: this is not the case for halos that emerged after $z = 6$ or not detected by the FOF. However this procedure guarantees that $t_{\rm prog}$ is set by material already in place in the structure by $z > 6$.

2.5. *Particle-based predictions*

This set of predictions is based on the halo-membership of each DM particle at z=0. Once the list of particles that belong to a z=0 halo is established, their positions at $z > 6$ can be traced-back from snaphots and each particle is then being assigned a reionization time: it is defined as the earliest time $t(z_R)$ at which a particle belongs to an ionized cell in the reionization map . An average particle-based $\langle t_{\rm part} \rangle$ is assigned to each halo:

$$\langle t_{\rm part} \rangle = \frac{\sum_{\vec{x}_{\rm p0} \in {\rm halo}} t_{\rm reion}(\vec{x}_{\rm pR})}{\sum_{\vec{x}_{\rm p0} \in {\rm halo}} 1}, \quad (2)$$

where $\vec{x}_{\rm p0}$ and $\vec{x}_{\rm pR}$ are the $z = 0$ and $z = z_R$ particles positions.

This procedure is more difficult to set up as it requires to cross-match 8×10^9 DM particles with $\sim 20 \times 10^6$ z=0 halos to assign particles to their halos. However this technique assigns reionization times to all z=0 haloes, even the smallest ones. On the other hand, these reionization times drift to later times since diffuse material, presumably reionized at later times and/or accreted after the Reionization, is taken into account.

3. RESULTS

3.1. *Reionization times*

The Reionization times of z=0 halos are shown in Fig. 3. Depending on the methodology used, galaxies with $M_{z=0} > 10^{11} h^{-1} M_\odot$ reionize up to 500 Myrs

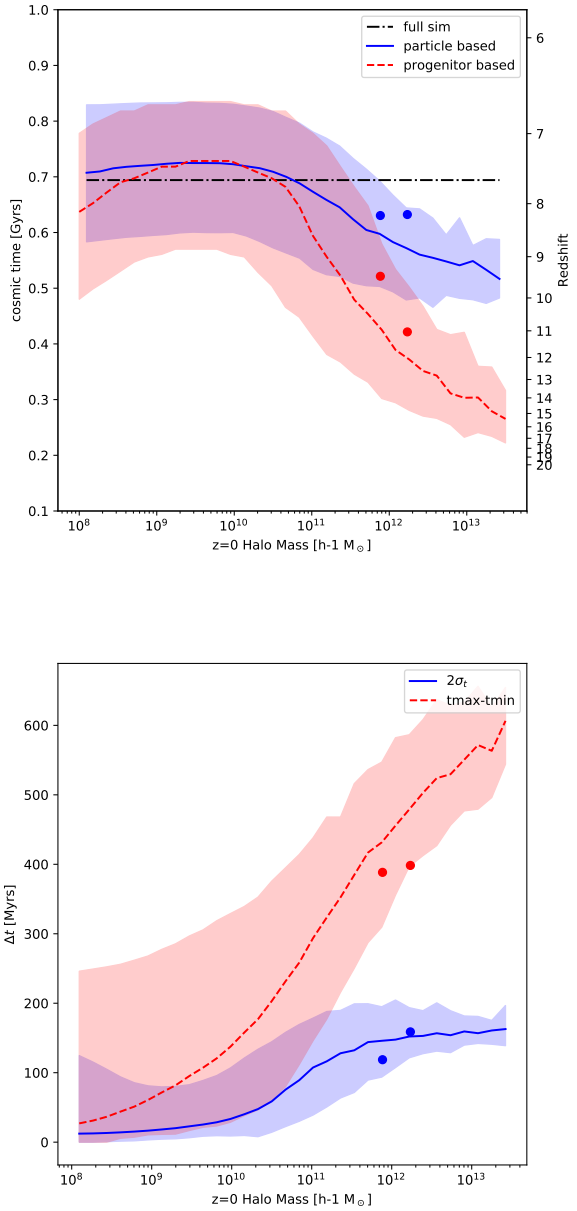

Figure 3. *Top*: The reionization time as a function of z=0 halo mass. The full volume reaches $x_{HI} = 0.5$ at $z \sim 7.8$ (dashed line). *Bottom*: The intrinsic duration of reionization Δt as a function of the halo mass. In both panels, lines stand for the median value within each bin of mass and shaded area cover the $5\% - 95\%$ percentiles. Dots stand for the measured values for the MW-M31 system analog. See text for the definitions of the different types of measurements.

earlier than the full volume. In this mass range, the more massive the galaxies, the earlier they are reionized as expected since they host intense sources or are close to them in dense environments. At the lower masses ($M_{z=0} < 10^{11} h^{-1} M_\odot$) the Reionization time becomes typically consistent with the global one. The median time is slightly later than the global one : objects among this population are faint or even star-less and must be externally reionized. Being dense, it takes more time to reionize them than for the IGM. Nevertheless, the scatter is significant from halo to halo ($\sim$ 250 Myrs 5%-95% percentile).

The two methodologies return consistent results but with differences. The progenitor-based technique guarantees that an object is already present at high z : it returns the reionization redshift of the oldest material of a z=0 halo, thus explaining why it consistently returns lower $t_{\rm reion}$. On the other hand it requires that FOF objects pre-exist at $z > 6$, biasing the sample of halos: a $10^8 h^{-1} M_\odot$ halo at z=0 must have peculiar accretion rates to have a $z > 6$ progenitor and still be light at z=0. The dip in reionization times at the low mass end confirms this and by eye inspection, these objects are located in high-density regions, thus explaining their low $t_{\rm reion}$. It could also indicate that these objects were more massive in the past and were stripped : these low-mass objects are being assigned $t_{\rm reion}$ typical of more massive objects.

The particle-based methodology suffers less from this bias because all z=0 halos are considered : the $t_{\rm reion}$ dip at the low-mass end disappears. It returns lower reionization redshifts for $M_{z=0} > 10^{11} M_\odot$, resulting from a fraction of material in halos at z=0 that was part of the diffuse matter in the IGM and was reionized at later times.

Li et al. (2014) found that $10^{12} h^{-1} M_\odot$ galaxies tend to reionize earlier than the IGM with $\Delta z \sim 1 \pm 1$ whereas we find earlier Reionization times for the same class of objects with $\Delta z \sim 1.5 \pm 1.5$ (particle-based) or $\Delta z \sim 4.5 \pm 3$ (progenitor-based). The differences could be related to methodologies : for instance they extrapolate reionization times using z=0 halos positions whereas we use $z > 6$ progenitors or particle positions. While their approximation is appropriate for halo masses with $> 10^{13} M_\odot$, we found that z=0 positions are a poor approximation of the actual halo position at high z when less massive objects are considered. Their reionization times closer to the global one could be a sign of 'signal dilution' at the lower-end of their probed range of halo mass.

3.2. *Durations of reionizations*

Using the particles reionization times, we can investigate the intrinsic reionization duration Δt of $t_{\rm reion}$ within halos : its dependance on halo mass is shown in Fig. 3. $\Delta t_{2\sigma}$ is computed from the r.m.s of par-

ticle reionization times within a halo, using $\Delta t_{2\sigma} = (\langle t_{\rm part}\rangle + \sigma) - (\langle t_{\rm part}\rangle - \sigma)$.

$\Delta t_{2\sigma}$ increases with the halo mass with typical values of $\sim$ 120 Myrs for $M_{z=0} > 10^{11}h^{-1}M_\odot$. For $10^{12}h^{-1}M_\odot$, reionization durations as long as 180 Myrs or as short as 60 Myrs can be found. Ocvirk et al. (2014) made similar measurements on subhaloes of M31-MW analogs and the current results are consistent with their SPH model that shares a similar emissivity for the sources: the 120 Myrs duration found here is typical of their Reionization in isolation models, where an inside-out Reionization proceeds from the inner regions of a galaxy to its outskirts. Meanwhile the shortest $\Delta t_{2\sigma} = 60$ Myrs values are typical of their external reionization scenario, where a nearby bright source 'flashes' the object. The scatter seen here would be a reflection of diverse environmental properties.

For $M_{z=0} > 10^{11}h^{-1}M_\odot$, the typical values found for $\Delta t_{2\sigma}$ are comparable to the halo-to-halo scatter of $t_{\rm reion}$ and are likely to be lower bound values since self-shielding is not fully taken into account at our resolution. It's consistent with findings of Alvarez et al. (2009) and Li et al. (2014) for more massive objects. Within a halo the Reionization is not instantaneous : it should be accounted by any model that includes the impact of local Reionization histories on stellar populations.

At low mass end, $M_{z=0} < 10^{11}h^{-1}M_\odot$, objects have $\Delta t_{2\sigma} \sim 0$. It corresponds to the extreme case of fast external reionizations or objects small enough to fit within a single cell of the Reionization map (the $30h^{-1}$ comoving kpc resolution corresponds to the virial radius of a $\sim 10^9h^{-1}M_\odot$ halo). The scatter increases toward the low mass end but these objects sampled with a small number of cells or particles (40 particles for $10^8h^{-1}M_\odot$) are poorly resolved by the AMR code. Their radiative environment history is not fully captured, with greater errors in the estimate of $\Delta t_{2\sigma}$.

Note that $\Delta t_{2\sigma}$ is an estimate of the duration to reionize most of the particles but time differences within a halo can be even greater.The time difference $\Delta t_{\rm max-min}$ between the first and the last particle to reionize is also given in Fig. 3. The most massive halos in our sample can have $\Delta t_{\rm max-min} = 600$ Myrs and thus contain material that saw its environment reionize at very different stages.

Lighter haloes have shorter $\Delta t_{\rm max-min}$ with $\Delta t_{\rm max-min} \sim$ 400 Myrs for $10^{12}h^{-1}M_\odot$ and $\Delta t_{\rm max-min} < 100$ Myrs for $M < 10^{10}h^{-1}M_\odot$. For this lightest class of objects, one can note that significant outliers are present, with $\Delta t_{\rm max-min} \sim 200$ Myrs when the median value is closer to 20 Myrs.

3.3. *The case of the Local Group*

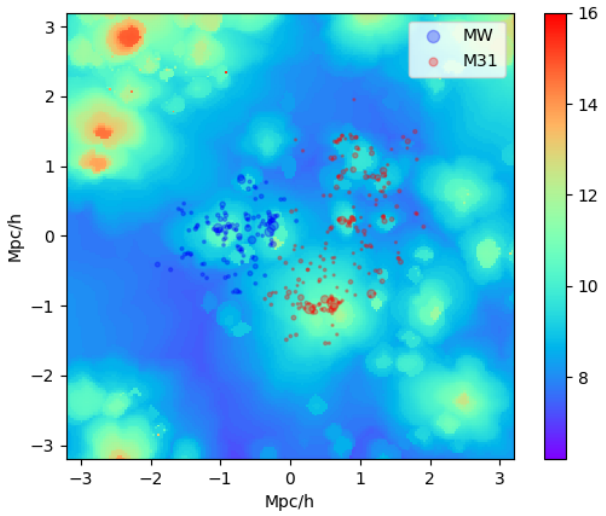

Figure 4. The EMMA reionization map around the LG (background field) and the location of GADGET halo progenitors at z=10.8 for the M31 and MW analogs (symbols). The size of the symbols are proportional to their masses. The background colors encode the reionization redshift.

The CLUES ICs lead to an analog of the LG at z=0 with two galaxies similar to the MW ($M_{z=0} = 7.7 \times 10^{11}h^{-1}M_\odot$) and M31 ($M_{z=0} = 1.7 \times 10^{12}h^{-1}M_\odot$) in the proper large-scale environment.

Fig. 4 shows the z=10.8 positions of their progenitors within the reionization map. The MW environment reionized in a compact fashion. Meanwhile M31 reionization pattern consists of several disconnected islands, reflecting the complex and extended distribution of progenitors at these times. Both objects reionized in isolation relative to each other: the patches are easily identified and disconnected. Ocvirk & Aubert (2011) and Gillet et al. (2015) predicted that it should lead to more extended radial distribution of satellites at z=0 compared to models without radiative transfer. The LG also reionized in isolation relative to the large scale environment, as no front sweep the region.

In fig. 3, their reionization times and durations are shown for each of the estimators. According to the progenitor-based method, M31 environment reionized earlier($z = 11$) than for MW ($z = 9.8$), in accordance with the measured trend where more massive haloes start their reionization earlier. Meanwhile the particle-based method indicates that both objects reionized at the same time, at $z = 8.2$: since these two objects are spatially close, it is not surprising that their lagrangian

environments reionized simultaneously. For both estimators, these two galaxies are typical of their respective class of masses, albeit on the 'late reionization' side of the distribution.

Regarding durations, $\Delta t_{2\sigma}$ are typical of the global distribution, between 100 and 150 Myrs. $\Delta t_{max-min} \sim$ 400 Myrs are similar for the two objects, an indication that their environments share similar extreme values for reionization times, presumably because of their closeness : it puts M31 reionization history among the most compact ones of its class of masses, maybe due to the proximity of the MW.

The particle-based durations and times are consistent with the partially suppressed model of Dixon et al. (2017) on the LG satellites, thus suggesting a modest but non-nil contribution of the low mass galaxies $M < 10^9 h^{-1} M_\odot$ to the Reionization in the CODA I-AMR.

4. PROSPECTS

The CODA I-AMR simulation and its combination to a CLUES DM simulation are the results of a long-term development strategy and challenging productions runs. Taken in conjunction with previous works, our results establish further the picture of an early, diverse and not instantaneous Reionization as seen by galaxies.

The models can be improved. For example, the inclusion of AGNs would lead to another sources of environmental fluctuations (see e.g. Chardin et al. (2015)), whereas models for star formation driven e.g. by molecular or metal cooling (see e.g. Wise & Cen (2009)) could modify the distribution of photons production among the halo classes. Likewise the volumes probed here are known to limit the representativity of HII regions sizes (see e.g. Iliev et al. (2006)) and underestimate the spatial fluctuation levels of Reionization fields. Also, the LG members reionized in isolation but it can be tested further using updated sets of constrained ICs (e.g. Carlesi et al. (2017)). These effects can modify our quantitative predictions, but we don't expect them to alter substantially our predictions.

Future investigations will include the environmental dependence of our results, as we expect field galaxies to experience the Reionization differently than members of groups or clusters. We also aim at investigating the detailed structure of the Reionization within haloes, with a focus on the impact on LG satellites.

PO and ND acknowledges support from the French ANR funded project ORAGE (ANR-14-CE33-0016). PRS acknowledges the grant support of NSF AST-1009799,NASA NNX11AE09G, and DOE INCITE 2016 Award AST031 on the Titan supercomputer at Oak Ridge National Laboratory. II is supported by the Science and Technology Facilities Council [grant numbers ST/F002858/1 and ST/I000976/1] and The Southeast Physics Network (SEPNet).The CoDA I-DM2048 simulation has been performed at LRZ Munich. GY would like to thank MINECO/FEDER (Spain) for financial support under research grant AYA2015-63810-P.

REFERENCES

Alvarez, M. A., Busha, M., Abel, T., & Wechsler, R. H. 2009, ApJL, 703, L167

Aubert, D., Deparis, N., & Ocvirk, P. 2015, MNRAS, 454, 1012

Bouwens, R. J., Bradley, L., Zitrin, A., et al. 2014, ApJ, 795, 126

Brown, T. M., Tumlinson, J., Geha, M., et al. 2014, ApJ, 796, 91

Busha, M. T., Alvarez, M. A., Wechsler, R. H., Abel, T., & Strigari, L. E. 2010, ApJ, 710, 408

Carlesi, E., Hoffman, Y., Sorce, J.,& Gottlber, S., 2017, MNRAS, 465, 4886

Chardin, J., Haehnelt, M. G., Aubert, D., & Puchwein, E. 2015, MNRAS, 453, 2943

D'Aloisio, A., McQuinn, M., Trac, H. 2015,ApJL, 813, L38

Davies, F. B. and Furlanetto, S. R.,MNRAS, 460, 1328

Deparis, N., Aubert, D., Ocvirk, P., & Gillet, N. 2017, submitted,

Dixon, K.,Iliev, I.,Gottlöber, S. Yepes, G. ,et al. 2017,arXiv:1703.06140

Fan, X., Carilli, C. L., & Keating, B. 2006, ARA&A, 44, 415.

Finkelstein, S. L., Ryan, Jr., R. E., Papovich, C., et al. 2015, ApJ, 810, 71

Gillet, N., Ocvirk, P., Aubert, D., et al. 2015, ApJ, 800, 34

Gottloeber, S., Hoffman, Y., & Yepes, G. 2010, ArXiv e-prints, arXiv:1005.2687

Hinshaw, G., Weiland, J. L., Hill, R. S., et al. 2009, ApJS, 180,225

Iliev, I. T., Mellema, G., Pen, U.-L., et al. 2006, MNRAS, 369, 1625

Iliev, I. T., Moore, B., Gottlöber, S., et al. 2011, MNRAS, 413, 2093

Koposov, S. E., Yoo, J., Rix, H.-W., et al. 2009, ApJ, 696, 2179

Leitherer, C., Schaerer, D., Goldader, J. D., et al. 1999, ApJS, 123, 3.

Li, T. Y., Alvarez, M. A., Wechsler, R. H., & Abel, T. 2014, ApJ, 785, 134

Ocvirk, P., & Aubert, D. 2011, MNRAS, 417, L93

Ocvirk, P., Gillet, N., Aubert, D., et al. 2014, ApJ, 794, 20

Ocvirk, P., Gillet, N., Shapiro, P. R., et al. 2016, MNRAS, 463, 1462

Planck Collaboration, Ade, P. A. R., Aghanim, N., et al. 2015, ArXiv e-prints, 1502, arXiv:1502.01589.

Rasera, Y., & Teyssier, R., 2006, A&A, 445,1

Springel, V. 2005, MNRAS, 364, 1105

Weinmann, S., Maccio, A., Iliev, I., et al. 2007, MNRAS, 381,367

Wise, J. H., & Cen, R. 2009, ApJ, 693, 984